Fault detection using Enhanced Adaptive degrees of freedom χ2-statistics method for Linear systems with mixed uncertainties

Quoc Hung Lu, Soheib Fergani, Carine Jauberthie

Fault detection using Enhanced Adaptive degrees of freedom χ^2-statistics method for Linear systems with mixed uncertainties

Quoc Hung Lu * **Soheib Fergani** * **Carine Jauberthie** *

* *LAAS-CNRS, 7 avenue du Colonel Roche, 31400 Toulouse, France (e-mail: qhlu@laas.fr, sfergani@laas.fr, cjaubert@laas.fr).*

Abstract: This article is concerned with a fault detection enhancement method using *adaptive amplifier coefficients* (a.a.c.) concept. It is developed for linear systems with mixed uncertainties (stochastic and bounded uncertainties framework). The study provides, also, analysis and discussions about the applicability and the efficiency of the enhanced method to several sensors fault error types. Simulations on a vehicle bicycle model (validated by experimental tests on the Renault Megane) are presented to emphasize on the performances of the developed method.

Keywords: Adaptive Innovation-based method, Fault diagnosis, Adaptive amplifier coefficient, Automotive bicycle model.

1. INTRODUCTION

Within the control theory and its field of applications, fault detection is extremely important for all system engineering problems. It is also a crucial component of any system diagnosis scheme and has received a lot of attention recently. Reliable *fault detection and isolation* (FDI) is a first class requirement in many fields. Indeed, efficient (early and accurate) fault detection can help avoid dangerous scenarios (accidents, explosions,...) or improve productivity (reducing process activity loss such as leakage...). The *model-based approaches* are proven to provide good results and acceptable tradeoff between fault sensitivity and computational cost especially those based on residual generation (see Patton et al. (2013) and references within).

Many methods and techniques have been developed to meet these abundant requirements. Several methods for fault detection in dynamic systems are mentioned in Willsky (1976), including the *innovation-based* method in which a χ^2-statistic hypothesis testing was used. This method is applied appropriately with the standard Kalman filter (Kalman, 1960) to process the linear dynamic system with deterministic coefficient matrices. In Sainz et al. (2002), an approach to generate envelopes based on interval techniques of the modal interval analysis is proposed. Puig (2010) reviews the use of *set-membership methods* in fault diagnosis and fault tolerant control. It aims at checking the consistency between observed and predicted behaviour by using simple sets to approximate the exact set of possible behaviours. Also, the design of stable *interval observers* for linear systems with additive time-varying zonotopic input bounds is proposed in Raka and Combastel (2013). Interval state observers provide an estimate on the set of admissible values of the state vector at each instant of time. Ideally, the size of the evaluated set is proportional to the model uncertainty, thus interval observers generate the state estimates with estimation error bounds, similarly to Kalman filters, but in the deterministic framework. Main tools and techniques for design of interval observers are reviewed in this tutorial for continuous-time, discrete-time and time-delayed systems (see Efimov and Raïssi (2016))). In Efimov and Raïssi (2016) a survey on interval state observers that provide an estimate on the set of admissible values of the state vector at each instant of time is provided.

The efficiency of these strategies has attracted the attention of the industrial community. The automotive industry, especially, has given more attention to these methods and though many academic studies have tried to provide solutions within this field based on set membership FDI. In Meseguer et al. (2010) a fault diagnosis approach is proposed. It has been motivated by the problem of detecting and isolating faults of the Barcelona's urban sewer system limnimeters (level meter sensors). It is based on interval observers which improve the integration of fault detection and isolation tasks. Ifqir et al. (2018) reviews the problem of robust state estimation and unknown input interval reconstruction for uncertain switched linear systems. A design method for obtaining interval observers that provide guaranteed lower and upper bounds of the state and unknown inputs is applied to vehicle lateral dynamics estimation to show the effectiveness of the algorithms. Also, in Chen et al. (2020), an extended set-membership filter applied to the vehicle's longitudinal velocity, lateral velocity, and sideslip angle provides not only higher accuracy, but also can provide a 100% hard boundary which contains the real values of the vehicle states (compared to the Unscented Kalman Filter UKF-based approaches).

Recently, in Tran (2017), authors provided an approach based on a χ^2-statistics test whose *degrees of freedom* (d.f.) is fixed and predetermined thanks to a size of a widows in which the statistic is computed. This approach is an innovation-based method but it is modified and applied to interval residual context. Then, Lu et al. (2021) have proposed an *adaptive degrees of freedom χ^2-statistic* (ADFC) method to provide an improved solution for the

same problem (mixed uncertainty assumption, interval residual context) of the former. This development consists in investigations of interval analysis related to d.f. of the considered statistic and results in the use of the so called *adaptive amplifier coefficients* (a.a.c.).

In present paper, the main contribution is the development of an enhanced ADFC (eADFC) method by discussing different levels of a.a.c. used in the method. The Bicycle vehicle model, used as a benchmark, is presented in detail together with multiple simulation results of fault detection based on this model.

The paper is organized as follows. Section 2 provides useful notations, the linear discrete time dynamic system with potential sensor faults, the enhanced method also evaluation indicators. In Section 3, the application to fault detection based on the Bicycle vehicle model is presented, included detail presentations of the model, simulation settings and results. Section 4 is a conclusion.

2. ENHANCED METHOD

2.1 Notations

A real interval matrix $[X]$ of dimension $p \times q$ is a matrix with real interval components $[x_{ij}]$, $i \in \{1, ..., p\}$, $j \in \{1, ..., q\}$. Write $X \in [X]$ to indicate a point matrix $X = (x_{ij})$ belonging element-wise to $[X]$. Define:

$$\begin{aligned} \overline{X} &\equiv \sup([X]) \triangleq (\sup([x_{ij}])), \\ \underline{X} &\equiv \inf([X]) \triangleq (\inf([x_{ij}])), \end{aligned}$$

as element-wise operators applying to $[X]$ and then $\text{mid}([X]) \triangleq (\overline{X} + \underline{X})/2$, $\text{rad}([X]) \triangleq (\overline{X} - \underline{X})/2$, $\text{width}([X]) \triangleq \overline{X} - \underline{X}$. Define also the (convex) hull of two interval matrices $[X_1]$, $[X_2]$ of the same dimension as $\text{hull}\{[X_1], [X_2]\} \triangleq [\min\{\underline{X}_1, \underline{X}_2\}, \max\{\overline{X}_1, \overline{X}_2\}]$.

Basic interval operators $\diamond \in \{+, -, \times, \div\}$ defined in Jaulin et al. (2001) can be used to compute directly all operations $[u] \diamond [v]$ and $\alpha \diamond [u]$, for real intervals $[u]$, $[v]$ and $\alpha \in \mathbb{R}$, without any further approximation algorithm. Then, interval matrix computations are defined similarly to matrix computations using the basic operators while more general operators are constructed by means of inclusion function $[f]$ (Jaulin et al., 2001). In practice, the package Intlab Rump (1998) developed for Matlab (also existing in Octave and C/C++) is used for computations.

Denote $\mathbb{I}(x) = 1$ if the conditions x are true and $\mathbb{I}(x) = 0$ otherwise, $\text{mean}(x) = \sum_{i=1}^{n} x_i/n$, $\forall x \in \mathbb{R}^n$, and $S_+([M])$ the set of all positive semi-definite matrices belonging to an interval matrix $[M]$. The notation $p : l : q$ $(p \leq q)$ is used for a range from p to q with step l. For $l = 1$, we write $p : q$. A sequence of variables can be noted interchangeably as $w_1, ..., w_k$ or $w_1 : w_k$ or $w_{1:k}$.

2.2 Model

Consider the following linear discrete time dynamic system

$$\begin{cases} x_k = A_k x_{k-1} + B_k u_k + w_k \,, \\ y_k = C_k x_k + D_k u_k + v_k + f_k^s \,, \end{cases} \qquad k \in \mathbb{N}^*, \qquad (1)$$

where $x_k \in \mathbb{R}^{n_x}$ and $y_k \in \mathbb{R}^{n_y}$ represent respectively state variable and measure, $u_k \in \mathbb{R}^{n_u}$ input, $w_k \in \mathbb{R}^{n_x}$ and $v_k \in \mathbb{R}^{n_y}$ stochastic noises. $f_k^s \in \mathbb{R}^{n_y}$ is a sensor fault vector. Each of its components corresponds to a sensor fault. Thus, the fault vector f_k^s can be of the multiple or single error type. In the first type, some (or all) sensors cause errors which affect the y_k value for the corresponding components. In the second type, only one sensor causes errors and just the corresponding y_k component is affected.

Assumptions (H): The initial state x_0 is normally distributed with mean μ_0 and covariance P_0. w_k and v_k are centered Gaussian vectors with covariance Q_k and R_k. Matrices $A_k, B_k, C_k, D_k, Q_k, R_k, P_0$ and μ_0 are unknown and belong to given interval matrices $[A], [B], [C], [D]$, $[Q], [R], [P_0]$ and $[\mu_0]$ respectively. x_0, $\{w_{1:k}\}$ and $\{v_{1:k}\}$ are mutually independent.

System (1) with assumptions **(H)** is a quite general model adapted to a wide range of applications. In this system, parameter matrices are time varying, the uncertainty may result from different sources (system disturbances, measurement noises) and may be of different kinds (stochastic and bounded uncertainties).

To evaluate the fault detection performance, indicators introduced in Lu et al. (2021) are used. Assume that system (1) is applied for N iterations among which faults occur in an time interval $\mathcal{R}$ with length l $(0 \leq l \leq N)$. $\mathcal{R}$ may be an interval or union of them but is called hereafter an *error range* for simplicity. A detection signal is denoted by π_k. It has value 0 (no fault is detected) or 1 (a fault is detected). A *right detected signal* is a signal $\pi_k = 1$ with $k \in \mathcal{R}$ and a *false detected signal* is a signal $\pi_k = 1$ with $k \notin \mathcal{R}$. Then, the indicators are defined as follows:

+ *Detection Rate*: $\text{DR} = \sum_{k \in \mathcal{R}} \mathbb{I}(\pi_k = 1)/l \times 100\%$,
+ *False Alarm Rate*: $\text{FAR} = \sum_{k \notin \mathcal{R}} \frac{\mathbb{I}(\pi_k = 1)}{N - l} \times 100\%$,
+ *Efficiency*: $\text{EFF} = \text{DR} - \text{FAR}$,
+ *No detection rate*: $\text{NDR} = 100\% - \text{DR}$.

2.3 Enhanced Adaptive degrees of freedom χ^2-statistic (eADFC) method

The ADFC in Lu et al. (2021) is an innovation-based method but deals with interval residual

$$[r_k] = y_k - [C][\hat{x}_{k|k-1}] - [D]u_k.$$

$[r_k]$ is the difference between the obtained measure y_k and an interval estimate of the later. $[r_k]$ contains all admissible residuals r_k's computed according to assumptions **(H)**. $[\hat{x}_{k|k-1}] = [A][\hat{x}_{k-1|k-1}] + [B]u_k$ is the interval version of the *a priori estimate* $\hat{x}_{k|k-1}$ of the (standard) Kalman filter. The considered statistic is U_k (Algorithm 1) which can be expressed as a function of $\text{width}([r_k])$. Furthermore, U_k is an upper bound of all admissible χ^2 statistics $r_k^T S_k^{-1} r_k$ of n_y d.f. where S_k is the covariance of r_k. Therefore, Lu et al. (2021) considered U_k as a χ^2 statistic of $\kappa_k n_y$ d.f. with an a.a.c. chosen as

$$\kappa_k = \text{mean}\left\{\text{width}([r_k])\right\}. \qquad (2)$$

This enlarges the traditional χ^2 statistic whose d.f. is normally a positive integer. The enlargement is mathematically legal thanks to the continuity of the χ^2 cumulative distribution function in its argument and parameter.

In general, we claim that :

- the choice of κ_k is not unique,
- there exists a better/optimal choice of κ_k for each of different applications (due to its intrinsic conditions),

- any choice of κ_k depends on predetermined purposes, e.g. control the system using u_k as control input or maintain the FAR below a target (5% for instance).

Therefore, in the present paper, we do not aim to provide a generic solution of the optimal choice of κ_k, nor to solve this problem in some specific cases. Instead, a flexible enhanced method is proposed by controlling the κ_k strength using a level parameter $\lambda_k > 0$. The controlled a.a.c. is now expressed as:

$$\kappa_k = \lambda_{\mathbf{k}} \cdot \text{mean}\left\{\text{width}([r_k])\right\}. \tag{3}$$

The method is simple and meaningful, since the κ_k of (2) is shown in Lu et al. (2021) to be chosen reasonably according to analysis of the statistic U_k, i.e. κ_k is sensitive to the fault, large enough to obtain a small FAR (e.g. $\leq$ 5%) in the fault free case, sensitively affected by width($[r_k]$) as well as U_k but it does not increase as fast as the later whenever a fault occurs and affects on the width($[r_k]$). This choice also provides a good performance fault detection with FAR $<$ 3% in several scenarios of simulations. Thus, the κ_k of (3) is raised naturally and its different controlled levels can be easily adapted to different applications and purposes.

In addition, we let open the choice of a.a.c. for designers but provide some guidelines and propositions as follows:

P1) *Constant level.* This is the most simple use of the level parameter, in which $\lambda_k \equiv c$, $\forall k \geq 1$, and $c > 0$ is determined experimentally by simulating many scenarios of the considered application. The best value of c according to some criteria is chosen.

P2) *Piece-wise constant level.* This is an advanced version of P1, in which $\lambda_k \equiv c_i$, for $N_i < k \leq N_i + M$, $c_i > 0$, $\{M, N_i, i\} \subset \mathbb{N}$ and $N_0 = 0$. The levels c_i can be determined such that FAR computed after every M time instants is bounded in some range $[\underline{x}, \overline{x}]$. Once FAR is smaller than $\underline{x}$ the level must be increased and vice-versa. Other criteria can be proposed to determined the level parameters.

The approach P1 is necessarily implemented off-line in the design stage while the approach P2 is apt to be implemented online to provide updated λ_k's after every delay of M time instants. This online procedure can be effectuated by using simultaneously two eADFC detectors as shown in Fig. 1. Indeed, the first detector aims at generating the detection signals for the system. The second one consists in providing an updated level λ_k by computing FAR indexes and using virtual faults f_k^{test}.

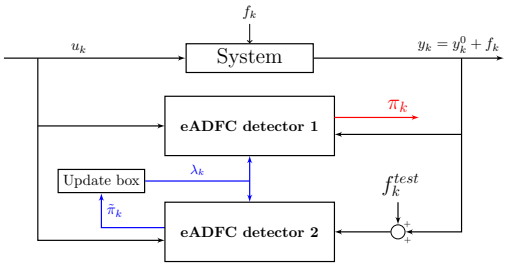

Fig. 1. General eADFC piece-wise constant level implemention diagram

Finally, the adjusting procedure of Algorithm 1 is important to enhance the fault detection method. It can help to reduce the FAR index by considering that in a window of size W (before or after time instant k), if the number of consecutive detected faults is not beyond W, then these faults (if exist) don't cause serious effects and will be dismissed. More precisely, π_k is kept its value 1 if $\sum_{i=k-W+1+j}^{k+j} \pi_i = W$ for $j = 0$ or $j = W-1$, which is expressed equivalently by line 14 of Algorithm 1.

The enhanced method is summarized and presented by Algorithm 1 in the following.

Algorithm 1 eADFC method

1: **Initialization:** $[\hat{x}_{0|0}], \mathcal{P}_{0|0}$, $[A], [B], [C], [D], [Q], [R]$, α, $\lambda_{\mathbf{k}}$, W, u_k, y_k, $k = 1, 2, ..., N$.
2: **for** $k = 1, 2, 3, ...N$ **do**
3: Compute: $[\hat{x}_{k|k-1}]$ and $[P_{k|k-1}]$ using OUBIKF (Algo.1 in Lu et al. (2021)).
4: $[r_k] = y_k - [C][\hat{x}_{k|k-1}] - [D]u_k$
5: $[S_k] = [C][P_{k|k-1}][C]^T + [R]$
6: Find a_k s.t. : $S_+([S_k]) \preceq a_k I$ using Theorem 2 in Lu et al. (2021).
7: $U_k = \sup\{\text{abs}([r_k]^T[r_k]/a_k)\}$
8: $\kappa_k = \lambda_{\mathbf{k}} \cdot \text{mean}\left\{\text{width}([r_k])\right\}$
9: Find δ_k s.t.: $\mathbb{P}(\chi^2(\kappa_k n_y) > \delta_k) = \alpha$.
10: Detection signal : $\pi_k = \mathbb{I}(U_k > \delta_k)$.
11: **end for**
Adjusting procedure:
12: Let $\pi_{k=1:N+2W} \leftarrow [\mathbf{0}_{1\times W}, \pi_{k=1:N}, \mathbf{0}_{1\times W}]$
13: **for** $k = 1 + W, ..., N + W$ **do**
14: $\pi_k \leftarrow \text{or}\left(\mathbb{I}\left(\sum_{i=k-W+1}^{k} \pi_i = W\right), \mathbb{I}\left(\sum_{i=k}^{k+W-1} \pi_i = W\right)\right)$
15: **end for**
16: $\pi_{k=1:N} \leftarrow \pi_{k=1+W+\lfloor W/2 \rfloor : N+W+\lfloor W/2 \rfloor}$

Notes: $0 < \alpha < 1$, $\lambda_k > 0$, $W \geq 1$.

3. APPLICATION

In this section, the efficiency of the proposed method is highlighted using a vehicle model validated on a real car.

3.1 Bicycle model

The vehicle model parameters obtained by an identification process on the Renault Mégane Coupé are presented. Indexes $i = \{f, r\}$ and $j = \{l, r\}$ are used to identify vehicle front, rear and left, right positions, respectively. The full vehicle model with the nonlinear equations describing its dynamical behaviour can be found in Fergani (2014).

Since the full model is highly nonlinear, a linear bicycle model as illustrated by Fig. 2 reproducing the lateral behaviour of the car is used for this study by linearizing the former. Reference to Fig. 2, $\beta(t)$ is the sideslip angle and $\psi(t)$ is the vehicle yaw which form the model state variables. $F_{ty_f}(t)$ represents lateral front tire forces, $F_{ty_r}(t)$ represents lateral rear tire forces and $F_{tx_f}(t)$ represents the longitudinal front tire forces, v is the vehicle speed, $\Delta F_{tx_r(t)}$ is the differential rear braking force (obtained based on the braking torques $T_{b_{rj}}$), δ is the steering angle and M_{dz} is the yaw moment disturbance.

The model is obtained considering the following: a) Low sideslip angles: $|\beta| < 7$ degrees, b) Low longitudinal slip ratio: < 0.1, c) Low steering angles: $\cos(\delta) \simeq 1$.

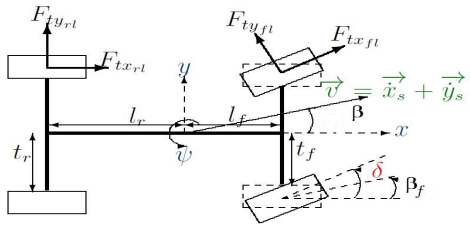

Fig. 2. View of the bicycle model reproducing the lateral behaviour of the car.

The linearized lateral tire forces are:

$$F_{ty_f}(t) = C_f\beta_f(t), \quad F_{ty_r}(t) = C_r\beta_r(t), \tag{4}$$

with the front and rear sideslip angles $\beta_f(t)$ and $\beta_r(t)$:

$$\beta_f(t) = \delta(t) - \beta(t) - \frac{l_f\dot{\psi}(t)}{v}, \quad \beta_r(t) = \beta(t) + \frac{l_f\dot{\psi}(t)}{v}. \tag{5}$$

This leads to the following state space representation (6):

$$\begin{bmatrix} \dot{\beta}(t) \\ \ddot{\psi}(t) \end{bmatrix} = \begin{bmatrix} \frac{-C_f - C_r}{mv} & 1 + \mu\frac{-l_rC_r - l_fC_f}{mv^2} \\ \frac{-l_rC_r - l_fC_f}{I_z} & \frac{-l_f^2C_f - l_r^2C_r}{I_zv} \end{bmatrix} \begin{bmatrix} \beta(t) \\ \dot{\psi}(t) \end{bmatrix} + \begin{bmatrix} \frac{C_f}{mv} & 0 & 0 & 0 \\ \frac{l_fC_f}{I_z} & \frac{1}{I_z} & \frac{S_rRt_r}{2I_z} & -\frac{S_rRt_r}{2I_z} \end{bmatrix} \begin{bmatrix} \delta \\ M_{dz} \\ T_{b_{rl}} \\ T_{b_{rr}} \end{bmatrix}. \tag{6}$$

Remark 1. The sideslip dynamics are highly nonlinear. They cannot be measured thanks to conventional sensors. μ is the tire/road adhesion coefficient. It takes value in $[0, 1]$ depending on the road conditions (dry, wet, icy,...) and influences strongly the vehicle lateral dynamics.

3.2 Simulation

The discretization of the model is performed with a time period $T = 0.05s$. Then, point matrices A, B, C, D are obtained and interval matrices $[A]$, $[B]$, $[C]$, $[D]$ are generated as follow: for $M \in \{A, B, C, D\}$, let $M = \text{mid}([M])$ and choose the radii $\text{rad}([M])$ at random in $[0\,, 0.5]$. The covariance matrices $[Q]$ and $[R]$ are generated in the same way by noting that their diagonal elements must be intervals of positive real numbers.

Inputs u_k's are simulated according to a dynamic change for $N = 864$ time instances, i.e. the vehicle is assumed to be driven at 15 m/s on a dry road ($\mu = 1$) and a double line change maneuver is performed from $t = 0.5$s to $t = 1.5$s by the driver. The initial state is chosen at $x_0 = (0, 0)^T$. For every k, choose at random A_k, B_k, C_k, D_k, Q_k, R_k in corresponding interval matrices and so that $Q_k \succeq 0$ and $R_k \succeq 0$. Then, $w_k \sim \mathcal{N}(0, Q_k)$, $v_k \sim \mathcal{N}(0, R_k)$ are simulated and $\{x_{1:N}, y_{1:N}\}$ are computed according to (1).

Sensor faults are generated in terms of additive vectors $f_k^s \in \mathbb{R}^{n_y}$. Let $b, b' \in \mathbb{R}$ be constant fault values, following types of error will be handled in the remaining:

Type 1: $f_k^s = b.\mathbf{1}$ where $\mathbf{1}$ is the all-ones vector in $\mathbb{R}^{n_y}$.
Type 2: $f_k^s = b.\mathbf{e_j}$ where $\mathbf{e_j}$ is the j-th column of the identity matrix I_{n_y}.
Type 3: $f_k^s = b.\mathbf{e_j} + b'.\mathbf{e_{j'}}$, with $j \neq j'$.

The error terms are added to y_k for all k in a range $\mathcal{R}$ with length l, i.e. $\mathcal{R} = r : r + l - 1$ for $r \in \{1 : N - l + 1\}$. Every sequence $\{y_{1i}, y_{2i}, ..., y_{Ni}\}$, with $i \in \{1, ..., n_y\}$, is called a chain. So, the errors occurred on multiple chains of y_k in type 1 and type 3 and only on single chain j in type 2.

Algorithm 1 is applied with following initializations: $\alpha = 0.05$, $W = 5$, $[\hat{x}_0] = ([-0.5, 0.5], [-0.5, 0.5])^T$, $\mathcal{P}_{0|0} = \max\{\text{diag}(\sup([Q]))\}I = 0.4412\,I$, upper bounds $\omega_k I$ of any set $S_+([M])$ identified by $\omega_k = \|\text{Max}([M])\|_F$ (Frobenius norm) where $[M] = ([m_{ij}])$ and $\text{Max}([M]) = (\max_{ij})$ so that $\max_{ij} = \sup([m_{ij}])$ if $\text{mid}([m_{ij}]) \geq 0$ and $\max_{ij} = \inf([m_{ij}])$ otherwise.

3.3 Results using identity level parameter $\lambda_k \equiv 1$

First results. A result of fault detection using eADFC method for type 1 of error with fault value $b = 20$ is shown in Fig. 3. The error range $[722 : 772]$ is between the two vertical black lines. The detection signals are very well determined.

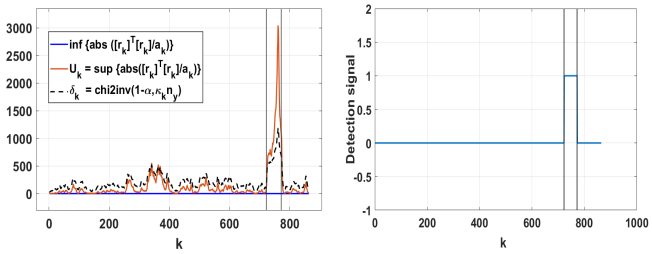

Fig. 3. eADFC method-Fault detection for Bicycle model.

A comparison between the proposed method and a fixed d.f. χ^2 fault detection strategy shows the importance of the adaptive characteristic of the approach. The method proposed in Tran (2017) (called Method A in the following) uses the statistic $T_k = \inf([r_k]^T\mathcal{S}_k^{-1}[r_k])$ with $S_+([S_k]) \preceq \mathcal{S}_k$. In this method, a fault is detected if $T_k > \delta$ where δ is determined by $\mathbb{P}(\chi^2(Wn_y) > \delta) = \alpha$. The first disadvantage of method A is that interval computation can let T_k be negative, consequently no fault is detected as illustrated in Fig.4 according to the bicycle model simulation. The second disadvantage is that a windows size W is arbitrarily chosen. An example can be built to illustrate this method works quite well (Fig.5 *Left*) in which T_k is non negative, but then the second disadvantage is still critical: another choice of W leads to another detection result. Our adaptive method in this case still provides an accurate fault detection (Fig.5 *Right*).

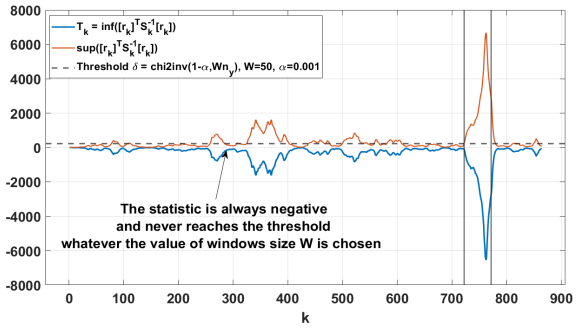

Fig. 4. Method A - Fault detection using statistic $T_k = \inf([r_k]^T\mathcal{S}_k^{-1}[r_k])$ for Bicycle model.

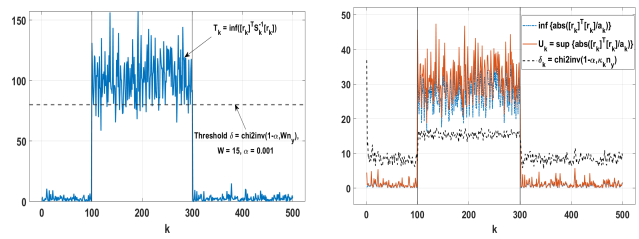

Fig. 5. Example-Fault detection with bias sensor fault $b = 10$: *(Left)*Method A, *(Right)* eADFC method.

Advanced results. Now, in order to survey, using eADFC method, how well the detection is when influencing factors are changed (e.g. fault values b and b', error range $\mathcal{R}$ and simulated variable y_k), indicators introduced in section 2 are used in following simulations. Three types of errors are simulated to get insight of the proposed method.

For this sake, the following **scenario setting** are used. Let f_k^s's be identical error vectors with k in an error range $\mathcal{R}$ whose length is $l = 50$. For each of different values of f_k^s, choose randomly error range $\mathcal{R}$ and do $L = 100$ times of y_k simulations and fault detections. Indicators are computed for each of L simulation times and their means are yielded afterward. Let $\tau_k = \max\{f_k^s\}/\text{Max\_width}$ where $\max\{f_k^s\}$ is the maximum component of f_k^s and Max_width is the maximum width of diagonal elements of $[Q]$ and $[R]$. This quantity provides an idea of how large is the maximum fault value with respect to some known quantity propagating through the dynamic system and affecting the measure values y_k, that is the maximum variance of noises.

Remark 2. This scenario is a combination of those scenarios presented in Lu et al. (2021), in which the error range or the y_k simulation is fixed.

Type 1 error. The sensor faults come to all chains of $\{y_k\}$, $f_k^s = b.\mathbf{1}$ and $\tau_k = \tau = b/\text{Max\_width}$ with $b = 0 : 5 : 30$.

Table 1. Fault detection for type 1 error.

b	τ	DR%	NDR%	FAR%	EFF%
0	0	1.48	98.52	1.53	-0.05
5	13.8	4.54	95.46	1.59	2.95
10	27.5	13.88	86.12	1.69	12.19
15	41.3	72.38	27.62	1.97	70.41
20	55.0	95.38	4.62	1.75	93.63
25	68.8	99.62	0.38	2.13	97.49
30	82.5	99.96	0.04	1.96	98.00

Type 2 error. The sensor faults only occur in one chain of $\{y_k\}$, $f_k^s = b.\mathbf{e_j}$ and $\tau_k = \tau = b/\text{Max\_width}$ with $b = 0 : 5 : 60$. The chain j on which the faults occur is chosen randomly at each of L times of y_k simulations. This situation corresponds to a single sensor and normally not all sensors are damaged at the same time. This situation is necessary for fault isolation in a further phase.

Type 3 error. Let $b = 10.m$ and $b' = 10.(m + 1)$ for $m = 1, 2, 3$. The chains j and j' at which the faults occur are also chosen randomly at each simulations. This setting, while still being of the multiple error type, can represent an intermediate situation between the settings of type 1 and type 2 error previously presented.

Table 2. Fault detection for type 2 error.

b	τ	DR%	NDR%	FAR%	EFF%
0	0	3.28	96.72	1.46	1.82
5	13.8	3.74	96.26	2.01	1.73
10	27.5	3.58	96.42	1.44	2.14
15	41.3	10.26	89.74	1.66	8.60
20	55.0	26.50	73.50	1.74	24.76
25	68.8	42.26	57.74	1.88	40.38
30	82.5	50.40	49.60	1.80	48.60
35	96.3	75.58	24.42	1.64	73.94
40	110.0	78.08	21.92	1.52	76.56
45	123.8	85.22	14.78	1.72	83.50
50	137.5	89.88	10.12	2.91	86.98
55	151.3	96.24	3.76	2.10	94.14
60	165.0	98.18	1.82	2.05	96.13

Table 3. Fault detection for type 3 error.

(b, b')	DR%	NDR%	FAR%	EFF%
(10,20)	42.84	57.16	5.29	37.55
(20,30)	79.38	20.62	5.33	74.05
(30,40)	98.82	1.18	5.59	93.23

The following remarks are valid for all three types of errors already simulated:

(R1) FAR does not vanish even in the fault free case ($b = 0$). This fact implies that there are other reasons (than fault) causing FAR. Actually, in this case, the error range degenerates to length 0, all 1-value detection signals are false detected signals, DR and NDR are not defined and FAR must be recomputed, e.g. according the first row of Table 1: $\text{FAR} = [1.53 \times (N - 50) + \ 1.48 \times 50]/N \approx 1.527$. However, we can think that b has a very small value and thus results in the Tables remain unchanged.

(R2) The negative value for EFF at $b = 0$ in Table 1 can be explained by the fact that, in this case, the fault detection procedure not only provides no efficiency gain, but rather a loss.

(R3) The factors causing FAR are multiple. Two of these factors that differ from simulations to simulations are random noises and random error ranges, which can therefore be called specific factors. Some other factors that exist for all simulations, and which can therefore be called general factors, are: the model performance (how well the model describes the dynamics of the vehicle), the interval computations, the lack of knowledge on the exact values of A_k, B_k, C_k,... and the performance of the χ^2-statistic test (with α significance level).

(R4) DR and EFF have ascending trends according to b values (or to $\max\{b, b'\}$) while FAR is rather stable in some range with positive values.

(R5) There is a threshold for good/bad result of EFF, e.g. $b \geq 15$ for type 1, $b \geq 35$ in type 2, $\max\{b, b'\} \geq 30$ in type 3.

(R6) The choice of significance level α is also a tunning factor for an appropriate fault detection.

3.4 Results for other constant level parameters λ_k

In this section, some other constant level parameters applied to Bicycle model are investigated. So, the performance of the eADFC method with constant level (P1) can be completely illustrated. The piece-wise constant level case (P2) is built straightforwardly from the former.

In the following simulations, $\lambda_k \equiv c$, $\forall k \geq 1$, with $c \in \{0.7, 0.3\}$. The simulation results are shown in Tables 4-5 in which only the type 2 error is concerned. Both cases of c are applied for common data samples.

Table 4. Fault detection for type 2 error using a.a.c κ_k with level parameter $\lambda_k \equiv 0.7$

b	τ	DR%	NDR%	FAR%	EFF%
0	0	5.84	94.16	4.39	1.45
5	13.8	5.88	94.12	4.62	1.26
10	27.5	13.30	86.70	4.58	8.72
15	41.3	29.52	70.48	4.42	25.10
20	55.0	53.56	46.44	5.01	48.55
25	68.8	68.10	31.90	3.99	64.11
30	82.5	77.94	22.06	3.84	74.10
35	96.3	85.08	14.92	4.43	80.65
40	110.0	94.12	5.88	4.71	89.41

.

Table 5. Fault detection for type 2 error using a.a.c κ_k with level parameter $\lambda_k \equiv 0.3$

b	τ	DR%	NDR%	FAR%	EFF%
0	0	24.64	75.36	25.14	-0.50
5	13.8	37.12	62.88	24.52	12.60
10	27.5	61.84	38.16	25.12	36.72
15	41.6	84.50	15.50	24.08	60.42
20	55.0	95.46	4.54	24.72	70.74
25	68.8	99.42	0.58	24.83	74.59
30	82.5	99.82	0.18	24.06	75.76
35	96.3	99.84	0.16	23.96	75.88
40	110.0	99.92	0.08	25.25	74.67

Tables 4 and 5 show that FAR increases when the level parameter λ_k decreases from 0.7 to 0.3. EFF also rises up for small values of b (< 35) according to the decrease of c.

When $c = 0.7$ (Table 4), the values of the FAR index disperse in $[3.8\,, 5.1](\%)$, and thus EFF = DR − FAR does not overpass 96.2% even if DR reaches its maximum value (100%). In addition, compared to Table 2 ($c = 1$), EFF increases considerably for many fault values $b < 35$ (starting at 10) and begins to achieve a remarkable rate (64.11%) starting at $b = 25$. Also in comparison with Table 2, but then the EFF does not increase in the case $b = 5$; this is due to the fact that Tables 2 and 4 display the simulation results of the different samples. The case $b = 0$ is not comparable (see remark (R1)).

When $c = 0.3$ (Table 5), the FAR range is $[23.9\,, 25.3](\%)$, EFF is never beyond 76.1%.

So, depending on the applications requiring a low FAR or a high EFF for a fine fault detection (detecting error with small fault value), different a.a.c κ_k can be chosen suitably thanks to the level parameters $\lambda_k > 0$.

4. CONCLUSION

An enhanced adaptive method to fault detection is proposed in this paper. The enhancement is presented in connection with the former method. The simplicity and efficiency of the method is highlighted from the design idea to the implementation perspective (as shown in the application simulations). The proposed method is well combined with the active fault diagnosis (AFD) approach developed in Lu et al. (2022).

REFERENCES

Chen, J., Guo, C., Hu, S., Sun, J., Langari, R., and Tang, C. (2020). Robust estimation of vehicle motion states utilizing an extended set-membership filter. *Applied Sciences*, 10(4), 1343.

Efimov, D. and Raïssi, T. (2016). Design of interval observers for uncertain dynamical systems. *Automation and Remote Control*, 77(2), 191–225.

Fergani, S. (2014). *Robust multivariable control for vehicle dynamics*. PhD thesis, Grenoble INP, GIPSA-lab, Control System dpt., Grenoble, France.

Ifqir, S., Ichalal, D., Oufroukh, N.A., and Mammar, S. (2018). Robust interval observer for switched systems with unknown inputs: Application to vehicle dynamics estimation. *European Journal of Control*, 44, 3–14.

Jaulin, L., Kieffer, M., Didrit, O., and Walter, E. (2001). *Applied Interval Analysis, with Examples in Parameter and State Estimation, Robust Control and Robotics*. Springer-Verlag, London.

Kalman, R. (1960). A new approach to linear filtering and prediction problems. *Transactions of the ASME–Journal of Basic Engineering*, 82(Series D), 35–45.

Lu, Q.H., Fergani, S., and Jauberthie, C. (2021). A new scheme for fault detection based on optimal upper bounded interval Kalman filter. *IFAC-PapersOnLine*, 54(7), 292–297. doi:https://doi.org/10.1016/j.ifacol.2021.08.374. 19th IFAC Symposium on System Identification SYSID2021.

Lu, Q.H., Fergani, S., and Jauberthie, C. (2022). Active fault diagnosis based on adaptive degrees of freedom x2-statistic method. In *2022 8th International Conference on Control, Decision and Information Technologies (CoDIT)*, volume 1, 843–848. doi:10.1109/CoDIT55151.2022.9804156.

Meseguer, J., Puig, V., and Escobet, T. (2010). Fault diagnosis using a timed discrete-event approach based on interval observers: Application to sewer networks. *IEEE Transactions on Systems, Man, and Cybernetics-Part A: Systems and Humans*, 40(5), 900–916.

Patton, R.J., Frank, P.M., and Clark, R.N. (2013). *Issues of fault diagnosis for dynamic systems*. Springer Science & Business Media.

Puig, V. (2010). Fault diagnosis and fault tolerant control using set-membership approaches: Application to real case studies. *International Journal of Applied Mathematics and Computer Science*, 20(4), 619–635.

Raka, S.A. and Combastel, C. (2013). Fault detection based on robust adaptive thresholds: A dynamic interval approach. *Annual Reviews in Control*, 37(1), 119–128.

Rump, S. (1998). Intlab - interval laboratory. *Developments in Reliable Computing*, 77–104.

Sainz, M.Á., Armengol, J., and Vehí, J. (2002). Fault detection and isolation of the three-tank system using the modal interval analysis. *Journal of process control*, 12(2), 325–338.

Tran, T. (2017). *Cadre unifié pour la modélisation des incertitudes statistiques et bornées - Application à la détection et isolation de défauts dans les systèmes dynamiques incertains par estimation*. Phd thesis, Université Toulouse III Paul Sabatier, LAAS, France.

Willsky, A.S. (1976). A survey of design methods for failure detection in dynamic systems. *Automatica*, 12, 601–611.